

Pair production of heavy $Q = 2/3$ singlets at LHC

J. A. Aguilar-Saavedra

*Departamento de Física and CFTP,
Instituto Superior Técnico, P-1049-001 Lisboa, Portugal*

Abstract

We examine the LHC discovery potential for new $Q = 2/3$ quark singlets T in the process $gg, qq \rightarrow T\bar{T} \rightarrow W^+b W^- \bar{b}$, with one W boson decaying hadronically and the other one leptonically. A particle-level simulation of this signal and its main backgrounds is performed, showing that heavy quarks with masses of 500 GeV or lighter can be discovered at the 5σ level after a few months of running, when an integrated luminosity of 3 fb^{-1} is collected. With a luminosity of 100 fb^{-1} , this process can signal the presence of heavy quarks with masses up to approximately 1 TeV. Finally, we discuss the complementarity among $T\bar{T}$, Tj production and indirect constraints from precise electroweak data in order to discover a new quark or set bounds on its mass.

1 Introduction

The Large Hadron Collider (LHC) will be a powerful tool to explore energies up to the scale of a few TeV. It is expected to provide some striking evidence of new physics, for instance of a light Higgs boson, in its first months of operation [1, 2]. Among many promising possibilities for the discovery of new particles, LHC will offer an ideal environment for the production of heavy quarks. New quarks of either charge can be copiously produced in pairs through QCD interactions, namely via gluon fusion and quark-antiquark annihilation, if there is available phase space [3, 4]. Up-type quarks T can also be produced in association with light jets, *e.g.* in the processes $qb \rightarrow q'T$, $\bar{q}'b \rightarrow \bar{q}T$ (here and throughout this Letter $q = u, c$, $q' = d, s$), provided their mixing with the bottom quark is sizeable. New interactions may also bring about further production mechanisms. The prospects for heavy quark detection depend on the production processes (with their respective cross sections) as well as on the decay modes (and their relevant backgrounds), which are distinctive of the Standard Model (SM) extension considered.

The presence of a fourth sequential generation is disfavoured by naturalness arguments¹ and precision electroweak data, which leave a small window for the new quark masses consistent with the experimental measurement of the S, T, U parameters [5]. On the other hand, heavy $SU(2)_L$ quark singlets with charges $Q = 2/3$ or $Q = -1/3$ can exist with a moderate mixing of order $10^{-2} - 10^{-1}$ with the SM quarks. Here we are concerned with the first possibility. Models with large extra dimensions with for example t_R in the bulk predict the existence of a tower of $Q = 2/3$ singlets $T_{L,R}^{(n)}$. If there is multilocalisation the lightest one, $T_{L,R}^{(1)}$ can have a mass of 300 GeV or larger, and a sizeable mixing with the top quark [6]. (The class of extra-dimensional models having a light $Q = 2/3$ singlet mixing with the top quark is enlarged when corrections localised on the branes to the kinetic terms of fermions and bosons are taken into account [7].) Little Higgs models [8] include in their additional spectrum an up-type singlet, which is expected to have a mass of 1 TeV or larger. Quark singlets also appear in some grand unified theories [4, 9]. Their effects in low energy and top physics have already been studied [10]. In this Letter we address their direct observation at LHC through pair production $gg, qq \rightarrow T\bar{T}$ [11].

We note that for heavy quark masses $m_T \gtrsim 800$ GeV and a coupling to the bottom quark V_{Tb} of the size suggested by the experimental measurement of the T parameter, single T production $pp \rightarrow Tj$ has a larger cross section than pair production and can then explore larger mass scales [12, 13]. Therefore, Tj production will eventually set more stringent limits (albeit dependent on V_{Tb}) on heavy quark masses if a positive signal is not observed. However, two important points have to be remarked: (i) the Tj cross section is proportional to $|V_{Tb}|^2$, hence for small mixings this process becomes less relevant; (ii) pair production has the best sensitivity to the presence of new quarks having masses of several hundreds of GeV. If new quarks exist in this mass range, $T\bar{T}$ production would allow to observe a signal in a rather short time.

In the following we briefly review the mixing of the new quark, its interactions and decay modes. After summarising the relevant aspects of the signal and background generation, we will present our results for quark masses of 500 GeV and 1 TeV. Finally, the relation between $T\bar{T}$, Tj production and indirect constraints from the T parameter will be discussed.

¹For a fourth quark generation, anomaly cancellation requires the simultaneous presence of a lepton doublet. LEP measurement of the Z invisible width sets the number of light neutrino species to three, and additional neutrinos must be heavier than 45 GeV [5], in sharp contrast with the smallness of the light neutrino masses $m_\nu \lesssim 1$ eV.

2 SM extensions with $Q = 2/3$ singlets

The addition of two $SU(2)_L$ singlet fields $T_{L,R}^0$ to the quark spectrum modifies the weak and scalar interactions involving $Q = 2/3$ quarks. (We denote weak eigenstates with a zero superscript, to distinguish them from mass eigenstates which do not bear superscripts.) Using standard notation, these interactions read

$$\begin{aligned}\mathcal{L}_W &= -\frac{g}{\sqrt{2}} [\bar{u}\gamma^\mu V P_L d W_\mu^+ + \bar{d}\gamma^\mu V^\dagger P_L u W_\mu^-] , \\ \mathcal{L}_Z &= -\frac{g}{2c_W} \bar{u}\gamma^\mu \left[X P_L - \frac{4}{3} s_W^2 \mathbb{1}_{4\times 4} \right] u Z_\mu , \\ \mathcal{L}_H &= \frac{g}{2M_W} \bar{u} [\mathcal{M}^u X P_L + X \mathcal{M}^u P_R] u H ,\end{aligned}\tag{1}$$

where $u = (u, c, t, T)$, $d = (d, s, b)$ and $P_{R,L} = (1 \pm \gamma_5)/2$. The extended Cabibbo-Kobayashi-Maskawa (CKM) matrix V is of dimension 4×3 , $X = VV^\dagger$ is a non-diagonal 4×4 matrix and \mathcal{M}^u is the 4×4 diagonal up-type quark mass matrix. The new mass eigenstate T is expected to couple mostly with third generation quarks t, b , because T_L^0, T_R^0 preferably mix with t_L^0, t_R^0 , respectively, due to the large top quark mass. V_{Tb} is mainly constrained by the contribution of the new quark to the T parameter [10, 14],

$$T = \frac{N_c}{16\pi s_W^2 c_W^2} \{ |V_{Tb}|^2 [\theta_+(y_T, y_b) - \theta_+(y_t, y_b)] - |X_{tT}|^2 \theta_+(y_T, y_t) \} ,\tag{2}$$

where $N_c = 3$ is the number of colours, $y_i = (\overline{m}_i/M_Z)^2$, \overline{m}_i being the $\overline{\text{MS}}$ mass of the quark i at the scale M_Z , $|X_{tT}|^2 \simeq |V_{Tb}|^2(1 - |V_{Tb}|^2)$ and [14]

$$\theta_+(y_1, y_2) = y_1 + y_2 - \frac{2y_1 y_2}{y_1 - y_2} \log \frac{y_1}{y_2} .\tag{3}$$

The experimental measurement $T = 0.12 \pm 0.10$ [15], obtained setting $U = 0$, implies $T \leq 0.28$ with a 95% confidence level (CL), and the corresponding limit $|V_{Tb}| \leq 0.26 - 0.18$ for $m_T = 500 - 1000$ GeV (see also Ref. [16]).² Mixing of T_L^0 with u_L^0, c_L^0 , especially with the latter, is very constrained by parity violation experiments and the measurement of R_c and $A_{\text{FB}}^{0,c}$ at LEP, respectively [17, 18], implying small X_{uT}, X_{cT} . The charged current couplings with d, s must be small as well, $|V_{Td}|, |V_{Ts}| \sim 0.05$, because otherwise the new quark would give large loop contributions to kaon and B physics observables [10]. Therefore, $|V_{Td}|, |V_{Ts}| \ll |V_{Tb}|$ and $|X_{uT}|, |X_{cT}| \ll |X_{tT}|$.

²The new quark contribution to U is much smaller, of order 10^{-2} [10], thus it makes sense using this value for T . If we take $T = -0.17 \pm 0.12$ [5] the limits obtained are much stronger, $T \leq 0.027$ and thus $|V_{Tb}| \leq 0.08 - 0.06$ for $m_T = 500 - 1000$ GeV. We will consider both possibilities in our analysis.

In specific models there may be additional interactions, *e.g.* mediated by new gauge bosons, giving further contributions to experimental observables. These extra terms might (partially) cancel the ones from the new quark, loosening the constraints on its couplings. Although new interactions may modify the allowed range for V_{Tb} , it is unlikely that they alter the above hierarchy. Then, the relevant decays of the new quark are $T \rightarrow W^+b$, Zt , Ht , with partial widths

$$\begin{aligned}
\Gamma(T \rightarrow W^+b) &= \frac{\alpha}{16 s_W^2} |V_{Tb}|^2 \frac{m_T^3}{M_W^2} \left[1 - 3 \frac{M_W^4}{m_T^4} + 2 \frac{M_W^6}{m_T^6} \right], \\
\Gamma(T \rightarrow Zt) &= \frac{\alpha}{16 s_W^2 c_W^2} |X_{tT}|^2 \frac{m_T^2}{M_Z^2} f(m_T, m_t, M_Z) \\
&\quad \times \left[1 + \frac{M_Z^2}{m_T^2} - 2 \frac{m_t^2}{m_T^2} - 2 \frac{M_Z^4}{m_T^4} + \frac{m_t^4}{m_T^4} + \frac{M_Z^2 m_t^2}{m_T^4} \right], \\
\Gamma(T \rightarrow Ht) &= \frac{\alpha}{16 s_W^2} |X_{tT}|^2 \frac{m_T^2}{M_W^2} f(m_T, m_t, M_H) \\
&\quad \times \left[1 + \frac{3}{4} \frac{m_t}{m_T} - \frac{1}{2} \frac{m_t^2}{m_T^2} - \frac{M_H^2}{m_T^2} + \frac{3}{4} \frac{m_t^3}{m_T^3} + \frac{m_t^4}{m_T^4} - \frac{m_t^2 M_H^2}{m_T^4} \right]. \quad (4)
\end{aligned}$$

The kinematical function

$$f(m_T, m_t, M) \equiv \frac{1}{2m_T} (m_T^4 + m_t^4 + M^4 - 2m_T^2 m_t^2 - 2m_T^2 M^2 - 2m_t^2 M^2)^{1/2} \quad (5)$$

approximately equals $m_T/2$ for $m_T \gg m_t, M$. For a heavy T and a light Higgs, we have $\text{Br}(T \rightarrow W^+b) \simeq 0.5$, $\text{Br}(T \rightarrow Zt) \simeq 0.25$, $\text{Br}(T \rightarrow Ht) \simeq 0.25$. To our knowledge, there are not experimental searches for new $Q = 2/3$ quarks giving lower bounds for their masses. However, for the expected production cross sections and decay branching ratios, it seems that quarks with masses around 200 GeV ought to be visible with present Tevatron Run II data [19].

The decays $T \rightarrow Zt \rightarrow \ell^+ \ell^- W^+ b$, $\ell = e, \mu$ give a cleaner final state than $T \rightarrow W^+ b$, but with a branching ratio 30 times smaller. It has already been found that the channel $T \rightarrow W^+ b$ ($\bar{T} \rightarrow W^- \bar{b}$), with $W \rightarrow \ell \nu$, gives the best discovery potential in single T production [12]. In $T\bar{T}$ production we select the final states $T\bar{T} \rightarrow W^+ b W^- \bar{b}$, with one W boson decaying leptonically and the other one hadronically. The larger cross section in this decay mode allows to obtain a better statistical significance for the signal, while the backgrounds can be greatly reduced with kinematical cuts.

3 Signal and background simulation

The main backgrounds for the $T\bar{T}$ signal

$$gg, qq \rightarrow T\bar{T} \rightarrow W^+ b W^- \bar{b} \rightarrow \ell^+ \nu b \bar{q} q' \bar{b}, \quad \ell = e, \mu \quad (6)$$

are given by $t\bar{t}$, $Wb\bar{b}jj$, $Zb\bar{b}jj$ and $t\bar{b}j$ production,

$$\begin{aligned} gg, qq &\rightarrow t\bar{t} \rightarrow W^+ b W^- \bar{b} \rightarrow \ell^+ \nu b \bar{q} q' \bar{b}, \\ pp &\rightarrow Wb\bar{b}jj \rightarrow \ell \nu b\bar{b}jj, \\ pp &\rightarrow Zb\bar{b}jj \rightarrow \ell^+ \ell^- b\bar{b}jj, \\ pp &\rightarrow t\bar{b}j \rightarrow W^+ b\bar{b}j \rightarrow \ell^+ \nu b\bar{b}j. \end{aligned} \quad (7)$$

The charge conjugate processes are understood to be summed in all cases. In the background evaluation we do not consider final states with τ leptons (which can decay leptonically $\tau \rightarrow e \nu_\tau \bar{\nu}_e$, $\tau \rightarrow \mu \nu_\tau \bar{\nu}_\mu$) because the electrons and muons produced in τ decays are softer, and in our analysis we eventually require e, μ with high transverse momenta. $Wjjjj$ and $Zjjjj$ production are reduced to negligible levels with the requirement of two b tags, which suppresses their contributions by a factor $\sim 10^{-4}$. The signal and the $t\bar{t}$, $t\bar{b}j$ backgrounds are evaluated with our own Monte Carlo generators, including all finite width and spin effects. We calculate the matrix elements using HELAS [20] with running coupling constants evaluated at the scale of the heavy quark T or t . $Wb\bar{b}jj$ and $Zb\bar{b}jj$ are calculated with ALPGEN [21]. The bottom quark mass $m_b = 4.8$ GeV is kept in all cases, and we take $M_H = 115$ GeV. We use structure functions CTEQ5L [22], with $Q^2 = \hat{s}$ for $T\bar{T}$, $t\bar{t}$ and $t\bar{b}j$, and $Q^2 = M_{W,Z}^2 + p_{T_{W,Z}}^2$ for $Wb\bar{b}jj$, $Zb\bar{b}jj$, being $\sqrt{\hat{s}}$ the partonic centre of mass energy, and $p_{T_{W,Z}}$ the transverse momentum of the gauge boson.³

The events are passed through PYTHIA 6.228 [24] as external processes to perform hadronisation and include initial and final state radiation (ISR, FSR) and multiple interactions. We use the standard PYTHIA settings except for b fragmentation, in which we use the Peterson parameterisation with $\epsilon_b = -0.0035$ [25]. A fast detector simulation ATLFast 2.60 [26], with standard settings, is used for the modelling of the ATLAS detector. We reconstruct jets using a standard cone algorithm with

³We find that $T\bar{T}$ cross sections are 16 – 18% larger (for $m_T = 500 - 1000$ GeV) when evaluated with MRST 2004 structure functions [23] and their corresponding value of $\alpha_s(M_Z)$. Assuming that background cross sections in the kinematical region of interest (large transverse momenta and invariant masses) scale by the same rate, this would amount to a 8 – 9% increase in the statistical significance.

$\Delta R \equiv \sqrt{(\Delta\eta)^2 + (\Delta\phi)^2} = 0.4$, where η is the pseudorapidity and ϕ the azimuthal angle. We do not apply trigger inefficiencies and assume a perfect charged lepton identification. The package **ATLFASTB** is used to recalibrate jet energies and perform b tagging, for which we select efficiencies of 60%, 50% for the low and high luminosity LHC phases, respectively.

4 Numerical results

The hadronised events are required to fulfill these two criteria: (a) the presence of one (and only one) isolated charged lepton, which must have transverse momentum $p_t \geq 20$ GeV and $|\eta| \leq 2.5$; (b) at least four jets with $p_t \geq 20$ GeV, $|\eta| \leq 2.5$, with exactly two b tags. The cross sections times efficiency of the five processes after these pre-selection cuts are collected in Table 1, using a 60% b tagging rate. The events are produced without kinematical cuts at the generator level in the case of $T\bar{T}$, $t\bar{t}$, while for the other processes we set some loose cuts, less restrictive than the ones used after hadronisation, which do not bias the calculation. For $t\bar{t}j$ we only require pseudorapidities $|\eta| \leq 3$ for b, j . For $Wb\bar{b}jj$ we set $p_t \geq 15$ GeV and $|\eta| \leq 3$ for the charged lepton, the b quarks and the jets, and lego-plot separations $\Delta R_{jj}, \Delta R_{bj}, \Delta R_{bb} \geq 0.4$, $\Delta R_{\ell b}, \Delta R_{\ell j} \geq 0.2$. For $Zb\bar{b}jj$ we require $p_t \geq 15$ GeV, $|\eta| \leq 3$ for b quarks and jets, $|\eta| \leq 10$ for the charged leptons, and $\Delta R_{jj}, \Delta R_{bj}, \Delta R_{bb} \geq 0.4$.

Process	$\sigma \times \text{eff}$
$T\bar{T}$ (500)	44.9 fb
$T\bar{T}$ (1000)	0.638 fb
$t\bar{t}$	18.8 pb
$Wb\bar{b}jj$	1.23 pb
$Zb\bar{b}jj$	246 fb
$t\bar{t}j$	710 fb

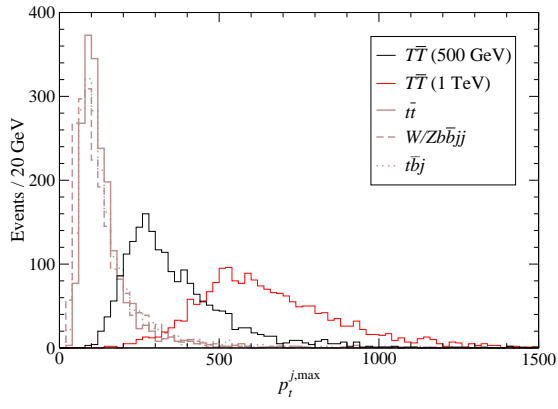
Table 1: Cross sections of the $T\bar{T}$ signal (with $m_T = 500, 1000$ GeV) and its backgrounds after pre-selection cuts.

The SM backgrounds are much larger than the signal, but they concentrate in the low transverse momenta region. To reduce them, it is useful to examine their dependence on the transverse momenta of the charged lepton p_t^{lep} , the fastest jet $p_t^{j, \text{max}}$ and the fastest b jet $p_t^{b, \text{max}}$, as well as the missing transverse momentum \cancel{p}_t and the

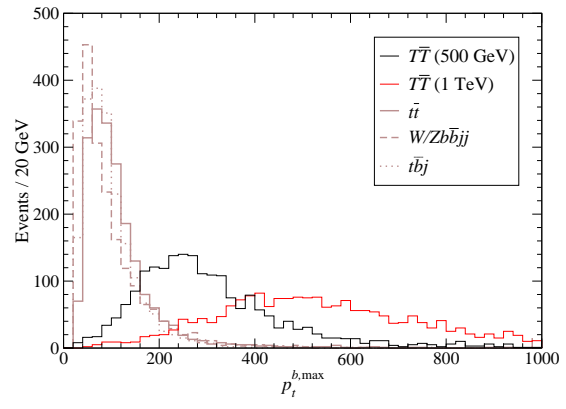
total transverse energy $H_t = \sum_{j,\ell,\gamma} p_t + \cancel{p}_t$. The kinematical distributions of these variables are shown in Fig. 1. We display a weighted sum of the $Wb\bar{b}jj$ and $Zb\bar{b}jj$ processes so as to reduce the number of histograms, while the other backgrounds are shown separately.

The $T\bar{T}$ signal can be discovered by the presence of peaks in the invariant mass distributions corresponding to the two decaying quarks. In order to reconstruct their momenta we first identify the two jets j_1, j_2 from the W decaying hadronically. The first one j_1 is chosen to be the highest p_t non- b jet, and the second one j_2 as the non- b jet having with j_1 an invariant mass closest to M_W . The missing transverse momentum is assigned to the undetected neutrino, and its longitudinal momentum and energy are found requiring that the invariant mass of the charged lepton and the neutrino is the W mass, $(p_\ell + p_\nu)^2 = M_W^2$. This equation yields two possible solutions. In addition, there are two different pairings of the two b jets to the W bosons decaying hadronically and leptonically, giving four possibilities for the reconstruction of the heavy quark momenta. We select the one giving closest invariant masses $m_T^{\text{had}}, m_T^{\text{lep}}$ for the quarks decaying hadronically and semileptonically. Their kinematical distributions are shown in Fig. 2. In our calculations we have set $V_{Tb} = 0.2, 0.1$ for $m_T = 500, 1000$ GeV, respectively, yielding the total widths $\Gamma_T = 2.80, 6.16$ GeV. The cross sections are independent of V_{Tb} and for Γ_T of these sizes the broadness of the mass distributions too.

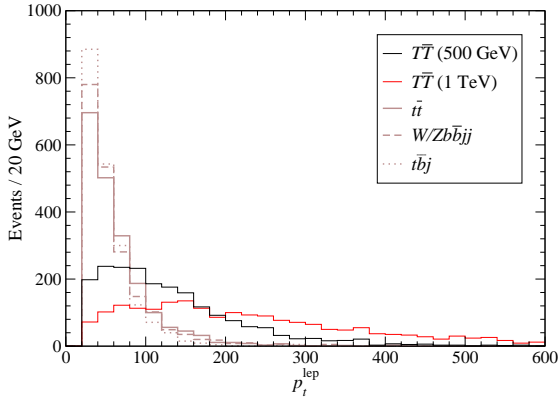
We point out that in our signal calculation we have not included other T production processes giving the same experimental signature of one charged lepton, four jets (with two b tags) plus missing energy. Such processes do not constitute a background (they are absent in the SM) but instead increase the signal cross section. One example is $T\bar{T}$ production in the decay channel $T\bar{T} \rightarrow ZtW^- \bar{b} \rightarrow \nu\bar{\nu}W^+bW^- \bar{b}$, with one W boson decaying hadronically and the other one leptonically. This process has a cross section 10 times smaller than the one in Eq. (6). Other possible $T\bar{T}$ decay channels are $T\bar{T} \rightarrow ZtW^- \bar{b} \rightarrow b\bar{b}W^+bW^- \bar{b}$, $T\bar{T} \rightarrow HtW^- \bar{b} \rightarrow b\bar{b}W^+bW^- \bar{b}$ (assuming a light Higgs boson) with two b quarks mistagged. Their contributions represent a $\sim 7\%$ and $\sim 40\%$ increase, respectively, in the total cross section. Nevertheless, neither of the three processes mentioned yields peaks in the $m_T^{\text{had}}, m_T^{\text{lep}}$ invariant mass distributions, as reconstructed here for the $T\bar{T} \rightarrow W^+bW^- \bar{b}$ signal, and their contributions are not likely to be detectable due to the uncertainty in the SM background normalisation. The same comments apply to $T\bar{b}j$ production with radiation of an extra hard jet.



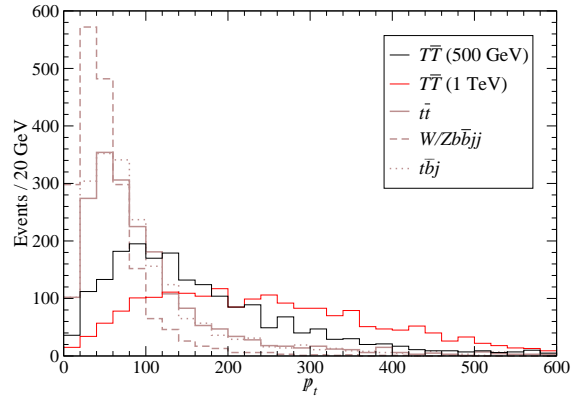
(a)



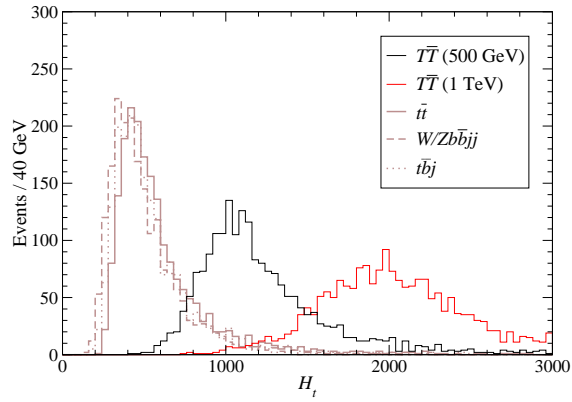
(b)



(c)



(d)



(e)

Figure 1: Transverse momentum of: (a) the fastest jet; (b) the fastest b jet; (c) the charged lepton. Missing transverse momentum (d); total transverse energy (e). The histograms are normalised to a total number of 2000 events.

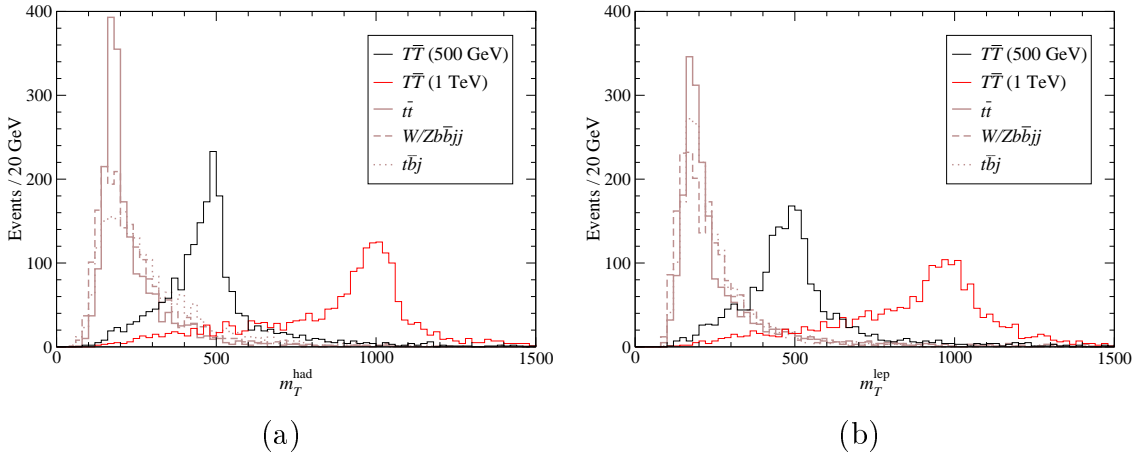


Figure 2: Reconstructed masses of the heavy quarks decaying hadronically (a) and semileptonically (b). The histograms are normalised to a total number of 2000 events.

4.1 Results for $m_T = 500$ GeV

The large background cross sections make it convenient to introduce further kinematical cuts at the generator level to reduce the number of events processed with **PYTHIA** and **ATLFAST**. We require the presence of a charged lepton with $p_t \geq 30$ GeV, a jet with $p_t \geq 200$ GeV and, for $Wb\bar{b}jj$ and $Zb\bar{b}jj$, one b quark with $p_t \geq 100$ GeV. This last cut does not bias the sample because in these two processes the two non- b jets mostly originate from light quarks and gluons, for which the b mistag probability is very low. Thus, the b -tagged jets correspond to the b quarks most of the time. The kinematical cuts used to reduce backgrounds are

$$\begin{aligned}
 p_t^{j,\max} &\geq 250 \text{ GeV}, & p_t^{b,\max} &\geq 150 \text{ GeV}, \\
 p_t^{\text{lep}} &\geq 50 \text{ GeV}, & 50 \text{ GeV} &\leq \cancel{p}_t \leq 600 \text{ GeV}, \\
 H_t &\geq 1000 \text{ GeV}.
 \end{aligned} \tag{8}$$

The cut $\cancel{p}_t \leq 600$ GeV is useful because $t\bar{t}$ production with large invariant masses is sometimes associated to very large \cancel{p}_t , in contrast with the signal. We also note that with these requirements the charged lepton and the hardest jet provide a trigger in the low luminosity LHC phase. The cross sections at the generator level are listed in the first column of Table 2, mainly for informative purposes. The second column represents the number of events $N_0 = K\sigma\mathcal{L}$ simulated, taking a luminosity of 10 fb^{-1} and including the rescaling factors K as explained in the appendix. The figures in these two columns corresponding to different processes should not be compared, since they

are obtained with different initial cuts in the event generation. Instead, the number of events N_{cut} surviving the selection criteria in Eq. (8) reflect the relative size of the processes after cuts. They are shown in the third column. (The size of the signals and backgrounds before cuts can be read from Table 1.)

Process	$\tilde{\sigma}$	N_0	N_{cut}	N_{peak}
$T\bar{T}$ (500)	204 fb	2700	272	173
$t\bar{t}$	5590 fb	70000	1609	240
$Wb\bar{b}jj$	928 fb	16000	287	65
$Zb\bar{b}jj$	364 fb	7200	39	10
$t\bar{t}j$	626 fb	8300	70	11

Table 2: For each process: cross sections $\tilde{\sigma}$ including cuts at the generator level; number of events simulated N_0 ; number of events N_{cut} passing the selection criteria in Eq. (8); number of events N_{peak} passing the selection cuts which are in the peak regions.

These kinematical cuts allow to detect the presence of the new quark in the invariant mass distributions m_T^{had} , m_T^{lep} as can be observed in Fig. 3. The number of events in the peak regions

$$340 \text{ GeV} \leq m_T^{\text{had}} \leq 660 \text{ GeV}, \quad 340 \text{ GeV} \leq m_T^{\text{lep}} \leq 660 \text{ GeV} \quad (9)$$

are displayed in the fourth column of Table 2. They give a statistical significance $S/\sqrt{B} = 9.6$. A 5σ significance, needed to claim discovery, can be achieved with a luminosity $\mathcal{L} \simeq 2.7 \text{ fb}^{-1}$. These numbers only consider statistical uncertainties, assuming that the SM background can be normalised with the cross section measurements outside the peak region in Eq. (9). Additionally, the trigger and charged lepton detection efficiencies must be taken into account, what reduces the statistical significance by a factor ~ 0.95 .

4.2 Results for $m_T = 1 \text{ TeV}$

We repeat the same analysis for a heavy quark with $m_T = 1 \text{ TeV}$, in this case choosing a b tagging rate of 50% at the high luminosity phase. The generator cuts are raised to $p_t \geq 150 \text{ GeV}$ for the charged lepton, $p_t \geq 250 \text{ GeV}$ for the hardest jet and $p_t \geq 150 \text{ GeV}$ for the hardest b quark, the latter cut only for $Wb\bar{b}jj$ and $Zb\bar{b}jj$ production. The parton-level cross sections for the five processes are listed in Table 3, together with the

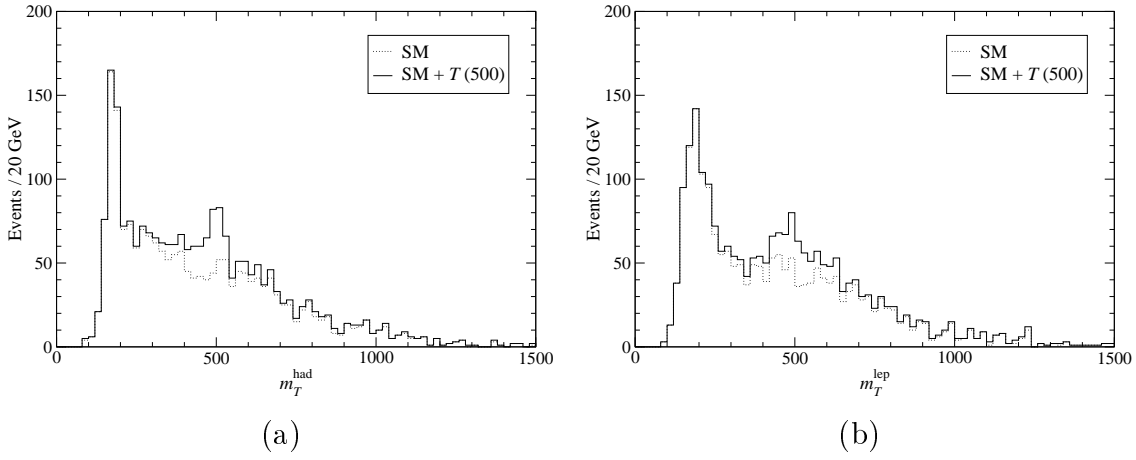


Figure 3: Reconstructed masses of the heavy quarks decaying hadronically (a) and semileptonically (b), after the selection cuts in Eq. (8). The dashed lines correspond to the SM predictions, while the full lines represent the SM plus a new 500 GeV quark.

number of simulated events N_0 , corresponding to an integrated luminosity of 300 fb^{-1} . The selection criteria used to reduce backgrounds are

$$\begin{aligned}
 p_t^{j,\max} &\geq 400 \text{ GeV}, & p_t^{b,\max} &\geq 300 \text{ GeV}, \\
 p_t^{\text{lep}} &\geq 200 \text{ GeV}, & 50 \text{ GeV} &\leq \cancel{p}_t \leq 400 \text{ GeV}, \\
 H_t &\geq 1800 \text{ GeV}.
 \end{aligned} \tag{10}$$

With these cuts the charged lepton and hardest jet provide a trigger for the event. The peak regions in this case are defined as

$$800 \text{ GeV} \leq m_T^{\text{had}} \leq 1200 \text{ GeV}, \quad 800 \text{ GeV} \leq m_T^{\text{lep}} \leq 1200 \text{ GeV}. \tag{11}$$

The invariant mass distributions m_T^{had} , m_T^{lep} after the cuts in Eq. (10) are shown in Fig. 4. The excess of events in the peak regions amounts to 9.4 standard deviations of the expected SM background. A 5σ significance would be achieved with an integrated luminosity $\mathcal{L} \simeq 85 \text{ fb}^{-1}$. With a simple rescaling it can be estimated that masses up to $m_T = 1.1 \text{ TeV}$ can be discovered with 5σ significance for $\mathcal{L} = 300 \text{ fb}^{-1}$ and, if no signal is found, the 95% CL limit $m_T \geq 1.3 \text{ TeV}$ can be set.

5 Summary and discussion

Up-type quark singlets with charge $Q = 2/3$ are predicted in some SM extensions, with masses ranging from few hundreds of GeV to several TeV. Their observation

Process	$\tilde{\sigma}$	N_0	N_{cut}	N_{peak}
$T\bar{T}$ (1000)	2.89 fb	1330	70	48
$t\bar{t}$	778 fb	294000	208	10
$Wb\bar{b}jj$	66.8 fb	34000	132	15
$Zb\bar{b}jj$	48.0 fb	28500	19	1
$t\bar{b}j$	44.1 fb	17500	3	0

Table 3: For each process: cross sections $\tilde{\sigma}$ including cuts at the generator level; number of events simulated N_0 ; number of events N_{cut} passing the selection criteria in Eq. (10); number of events N_{peak} passing the selection cuts which are in the peak regions.

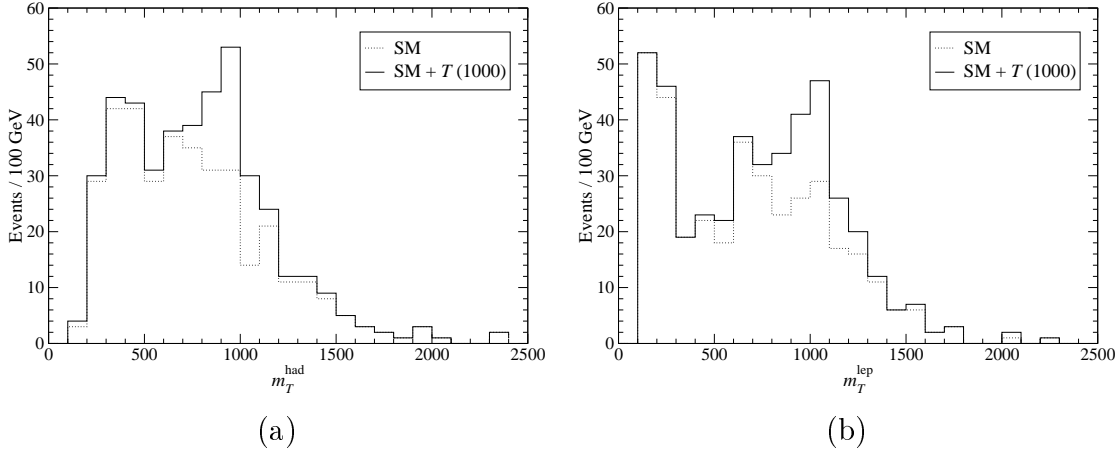


Figure 4: Reconstructed masses of the heavy quarks decaying hadronically (a) and semileptonically (b), after the selection cuts in Eq. (10). The dashed lines correspond to the SM predictions, while the full lines represent the SM plus a new 1 TeV quark.

would represent not only a clear new physics signal but also an important confirmation for these models. We have shown that for $m_T = 500$ GeV a 5σ statistical significance would be attained already with 3 fb^{-1} of integrated luminosity, which can be collected after few months of LHC operation in its first phase. For new quarks in this mass range, $T\bar{T}$ production provides the best signal of their presence, allowing a prompt discovery if they exist. With an integrated luminosity of 300 fb^{-1} , $T\bar{T}$ production may discover a new quark with $m_T \leq 1.1 \text{ TeV}$, or set a 95% CL bound $m_T > 1.3 \text{ TeV}$, independent of V_{Tb} , if no signal is observed.

We point out that if a fourth quark generation (T, B) exists with $m_T < m_B$ the dominant decay of the up-type quark is $T \rightarrow Wb$, giving the same signal studied

here. ($T \rightarrow Zt, Ht$ are forbidden at the tree level by the vanishing of the flavour-changing neutral coupling X_{tT} .) The results obtained for an up-type singlet can then be straightforwardly applied to a fourth generation quark, multiplying the statistical significances in section 4 by a factor of four. If $m_T < m_B$, a fourth generation quark T with $m_T \leq 1.3$ TeV could be discovered with 300 fb^{-1} of integrated luminosity, and the 95% CL bound $m_T > 1.5$ TeV could be set if they are not observed. If B is lighter than T , the decay $T \rightarrow W^+ B$, with W on its mass shell if $m_T > m_B + M_W$, is open. Hence, the branching ratio of $T \rightarrow Wb$ depends on V_{Tb} , and model-independent predictions cannot be made. We also remark that in case that a new quark T is discovered without a $Q = -1/3$ partner, the experimental search for the decays $T \rightarrow Zt, Ht$ can determine if T is a $\text{SU}(2)_L$ singlet or belongs to a doublet (in which case its partner B should be heavier and undetected).

New $Q = 2/3$ quark singlets can be produced in association with light jets as well, mainly in the processes $ub \rightarrow dT, d\bar{b} \rightarrow u\bar{T}$. The cross sections for Tj production are quadratic in $|V_{tb}|$, but on the other hand they do not decrease with m_T as quickly as for $T\bar{T}$. We plot in Fig. 5 (a) the cross sections for $T\bar{T}$ and Tj production for different heavy quark masses. For Tj we select a fixed coupling $V_{Tb} = 0.1$ as well as an m_T -dependent coupling suggested by the experimental central value $T = 0.12$ (obtained for $U = 0$) and Eq. (2). The V_{Tb} values derived from $T = 0.12$ are shown in Fig. 5 (b). Of course, in models beyond the SM there may be additional contributions to oblique corrections, thus we take the experimental measurement of T only as a hint on the size of V_{Tb} . In Fig. 5 (b) we also plot the Little Higgs model relation $V_{Tb} = m_t/m_T$ and the two 95% CL upper limits on $|V_{Tb}|$ obtained from

$$\begin{aligned} T &\leq 0.28 && (95\% \text{ CL}, U = 0), \\ T &\leq 0.027 && (95\% \text{ CL}, U \text{ arbitrary}), \end{aligned} \tag{12}$$

respectively. We note that the assumption $V_{Tb} = m_t/m_T$ potentially conflicts with the T parameter measurement for $m_T < 900$ GeV, even using the less restrictive bound $T \leq 0.28$.

The discovery potential of Tj production can be estimated from existing analyses. This process, with $T \rightarrow Wb \rightarrow \ell\nu b$, gives a 21.5σ significance for $m_T = 1$ TeV and $V_{Tb} = m_t/m_T \simeq 0.175$ [13]. We make the reasonable assumption that for different T masses the signal to background ratio S/B in the kinematical region of interest (with high p_t and invariant masses $\sim m_T$) remains approximately constant (obviously

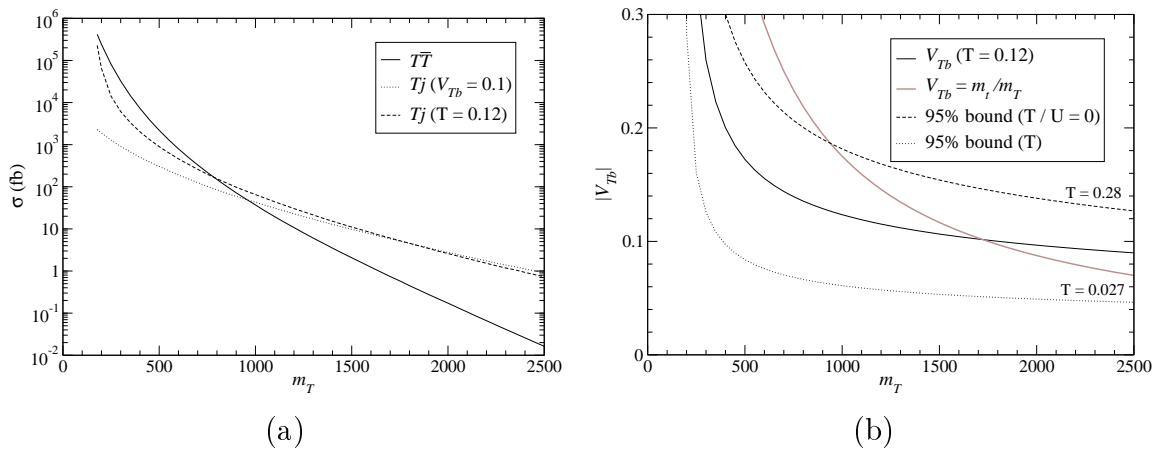


Figure 5: (a) Cross sections for $T\bar{T}$ production (full line) and Tj production, in the latter case for $V_{Tb} = 0.1$ (dotted line), and for V_{Tb} derived from the T parameter (dashed line). (b) Upper bounds on $|V_{Tb}|$ and values suggested by the T parameter (black line) and the Little Higgs relation $V_{Tb} = m_t/m_T$ (grey line).

keeping equal CKM factors $|V_{Tb}|^2$ for the signal).⁴ Requiring a statistical significance $S/\sqrt{B} = 5$ sets a lower limit on the coupling V_{Tb} for each m_T value. These limits are plotted in Fig. 6 (a), together with the discovery limit $m_T \leq 1.1$ TeV for T pair production. We also include the 95% CL bounds from the T parameter in Eq. (12). We point out that if $T \leq 0.027$ is enforced the discovery reach of $T\bar{T}$ production is higher than for Tj , since for $m_T \gtrsim 700$ GeV the V_{Tb} values needed for 5σ discovery in Tj production are not allowed. Assuming the less restrictive limit $T \leq 0.28$, there is a region (light shaded area in the figure) where the new quark can be discovered in single T but not in T pair production. Conversely, in the dark shaded area the new quark can be discovered in $T\bar{T}$ production but not in single T processes.

The discovery of a new $Q = 2/3$ quark singlet would certainly be a rather important achievement towards the understanding of the flavour structure of the SM, and might help explain the largeness of the top quark mass [8, 27]. On the other hand, the non-observation of new quarks at LHC would also be interesting on its own. In such case, the combined bounds obtained from single and T pair production and the T parameter would restrict m_T , $|V_{Tb}|$ to lie in the shaded area in Fig. 6 (b). (If we use the more

⁴This assumption is justified by the decrease of the tails in the transverse momenta and invariant mass distributions of the SM background. More optimistic extrapolations of the SM background cross section, *e.g.* assuming that it decreases faster than the Tj signal, would lead to higher discovery limits on T masses, as the ones given in Ref. [12].

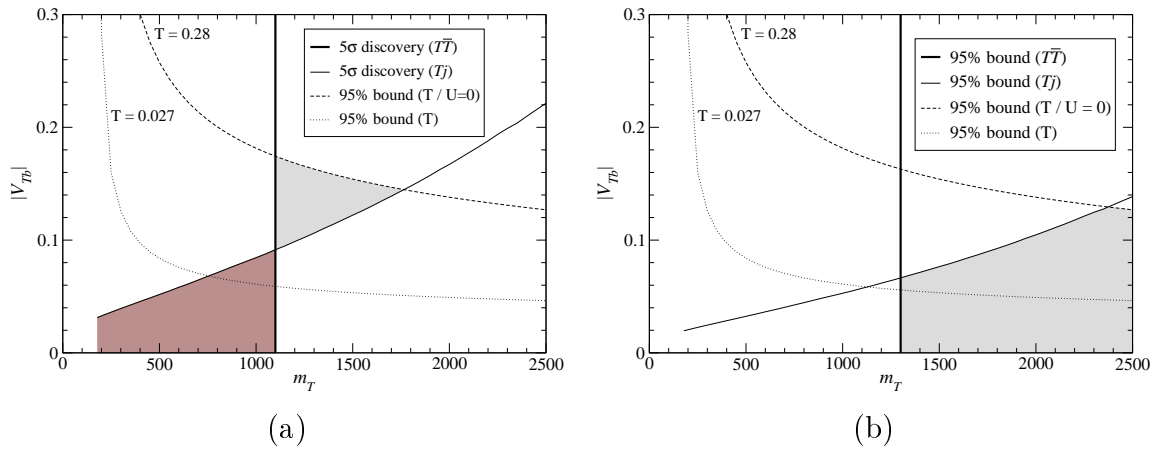


Figure 6: (a) 5σ discovery limits for the new quark (full lines), and indirect bounds from the T parameter, explained in the text. (b) Combined 95% CL bounds on m_T , $|V_{Tb}|$ (shaded area) from $T\bar{T}$, Tj production and the T parameter, if $Q = 2/3$ quark singlets are not observed at LHC.

restrictive bound in Eq. (12) the allowed region is somewhat smaller, as can be seen in the figure.) In this area we have $m_T \geq 1.3$ TeV and $|V_{Tb}| \leq 0.13$, the latter implying $|V_{tb}| \geq 0.991$. For $m_T \geq 600$ GeV, the couplings V_{Td} , V_{Ts} are already very constrained by kaon and B physics measurements [10]. Therefore, the non-observation of a new quark would significantly improve the indirect limits on CKM matrix elements V_{td} , V_{ts} , V_{tb} within this class of models.

Acknowledgements

I thank F. del Aguila and R. Pittau for useful discussions and a critical reading of the manuscript. This work has been supported by FCT through project CFTP-FCT UNIT 777 and grant SFRH/BPD/12603/2003.

A Appendix: signal and background normalisation

In addition to the processes listed in Eqs. (6),(7) there are other higher order processes contributing to the signal and backgrounds, namely final states including extra jets from QCD radiation. Indeed, $t\bar{t}j$ production only yields three jets at the partonic

level, and the fourth one required to pass our pre-selection criteria must be originated by radiation. These higher-order processes are approximately accounted for by **PYTHIA** showering, which generates hard extra jets by FSR. For example, in $Wb\bar{b}jj$ production some fraction of the events, when passed through **PYTHIA** showering, are converted into $Wb\bar{b}jjj$ or $Wb\bar{b}jjjj$ events, the additional jets with a high ($\gtrsim 50$ GeV) transverse momentum.

One possible method to take higher order processes into account is to generate them at the parton level, forbidding **PYTHIA** to radiate hard extra jets to avoid double counting [28] but allowing the soft and collinear ones. Instead, our approach is to normalise the numbers of events simulated N_0 by approximate correction factors K so that these figures correspond to the processes in Eqs. (6),(7) plus higher order ones. The number of events simulated for a given process is then $N_0 = K\sigma\mathcal{L}$, being σ the cross section of the process and \mathcal{L} the luminosity. The correction factor K is calculated in the $Wb\bar{b}jj$ example as follows:

1. We generate $Wb\bar{b}jj$ events requiring high transverse momenta $p_t \geq 100$ GeV for jets at the generator level, and a large separation $\Delta R \geq 0.6$ among all partons.
2. These events are passed twice through **PYTHIA** and **ATLFAST**, including FSR and without including it. In both cases ISR, multiple interactions and energy smearing are turned off, because we want to isolate the effect of FSR.
3. We examine the number of events with four-jets (corresponding to the four initial partons) with $p_t \geq 80$ GeV in both samples. Let us call these numbers n_4^0, n_4^{FSR} , respectively. K is then defined as the ratio between them, $K = n_4^0/n_4^{\text{FSR}}$.

With this rescaling factor definition, the number of four-jet events after FSR corresponds to the one present at the parton level. The value of K depends on the cut values for the event generation (100 GeV) and the jet counting (80 GeV), and therefore this procedure is approximate. However, for our purposes this simple and fast K -factor prescription seems sufficient. For the $T\bar{T}$ signal we obtain $K(T\bar{T}) \simeq 1.3$, $K(T\bar{T}) \simeq 1.5$ for heavy masses of 500 GeV and 1 TeV, respectively, and for the backgrounds $K(t\bar{t}) \simeq 1.3$, $K(t\bar{t}j) \simeq 1.3$, $K(Wb\bar{b}jj) \simeq 1.7$, $K(Zb\bar{b}jj) \simeq 2.0$.

References

- [1] ATLAS collaboration, Technical Design Report, CERN-LHCC-99-15; CMS Collaboration, Technical Proposal, CERN-LHCC-94-38
- [2] G. Weiglein *et al.* [LHC/LC Study Group], hep-ph/0410364
- [3] E. Eichten, I. Hinchliffe, K. D. Lane and C. Quigg, Rev. Mod. Phys. **56** (1984) 579 [Addendum-ibid. **58** (1986) 1065]
- [4] P. H. Frampton, P. Q. Hung and M. Sher, Phys. Rept. **330** (2000) 263
- [5] S. Eidelman *et al.* [Particle Data Group], Phys. Lett. B **592** (2004) 1
- [6] F. del Aguila and J. Santiago, JHEP **0203** (2002) 010
- [7] F. del Aguila, M. Perez-Victoria and J. Santiago, hep-ph/0305119; Acta Phys. Polon. B **34** (2003) 5511
- [8] N. Arkani-Hamed, A. G. Cohen and H. Georgi, Phys. Lett. B **513** (2001) 232
- [9] V. D. Barger, M. S. Berger and R. J. N. Phillips, Phys. Rev. D **52** (1995) 1663
- [10] J. A. Aguilar-Saavedra, Phys. Rev. D **67** (2003) 035003 [Erratum-ibid. D **69** (2004) 099901]
- [11] F. del Aguila, L. Ametller, G. L. Kane and J. Vidal, Nucl. Phys. B **334** (1990) 1
- [12] G. Azuelos *et al.*, Eur. Phys. J. C **39S2** (2005) 13
- [13] D. Costanzo, ATLAS note ATL-PHYS-2004-004
- [14] L. Lavoura and J. P. Silva, Phys. Rev. D **47** (1993) 2046
- [15] LEP Electroweak Working Group, Results Summer 2004: M. Grünewald, http://lepewwg.web.cern.ch/LEPEWWG/stanmod/summer2004_results
- [16] F. del Aguila and R. Pittau, Acta Phys. Polon. B **35** (2004) 2767
- [17] P. Langacker and D. London, Phys. Rev. D **38** (1988) 886
- [18] F. del Aguila, J. A. Aguilar-Saavedra and R. Miquel, Phys. Rev. Lett. **82** (1999) 1628

- [19] See for instance G. Gomez [CDF - Run II Collaboration], hep-ex/0505095
- [20] E. Murayama, I. Watanabe and K. Hagiwara, KEK report 91-11, January 1992
- [21] M. L. Mangano, M. Moretti, F. Piccinini, R. Pittau and A. D. Polosa, JHEP **0307** (2003) 001; See also <http://mlm.home.cern.ch/m/mlm/www/alpgen/>
- [22] H. L. Lai *et al.* [CTEQ Collaboration], Eur. Phys. J. C **12** (2000) 375
- [23] A. D. Martin, R. G. Roberts, W. J. Stirling and R. S. Thorne, Phys. Lett. B **604** (2004) 61
- [24] T. Sjostrand, P. Eden, C. Friberg, L. Lonnblad, G. Miu, S. Mrenna and E. Norrbin, Comput. Phys. Commun. **135** (2001) 238
- [25] R. Barate *et al.* [ALEPH Collaboration], Phys. Rept. **294** (1998) 1
- [26] E. Richter-Was, D. Froidevaux and L. Poggioli, ATL-PHYS-98-131
- [27] F. del Aguila and M. J. Bowick, Nucl. Phys. B **224** (1983) 107
- [28] M. Mangano, talk at the workshop “*Monte Carlo for Run 2*”, FNAL, June 2004, <http://cepa.fnal.gov/patriot/mc4run2/MCTuning/061104/mlm.pdf>